THE ORIGIN OF THE LOW-T HELICAL STATE AND THE FIELD-INDUCED PHASE TRANSITIONS IN THE REENTRANT SUPERCONDUCTOR $HoNi_2B_2C$.

M. El Massalami and E.M.Baggio-Saitovitch.

CBPF, R.Xavier Sigaud 150, 22290-180, Rio de Janeiro, Brazil

ABSTRACT

Longitudinal magnetoresistivity of textured polycrystalline $HoNi_2B_2C$ in the reentrant region (T = 4.7(2) K, 0 < H< 80 kOe) shows a cascade of field-induced magnetic phase transitions. These transitions (and the reported H-T phase diagram) are interpreted as follows: for $T < T_N$, an external field ($>H_{c2}$) first transforms the superconducting antiferromagntic ground state into a non-superconducting distorted helical state. This distorted helical state is transformed (on further field increase) into the ferromagnetic state via two types of fan-like spin-structures. On the other hand, the formation of the helical state is attributed to the competing character of the RKKY-type antiferromagnetic couplings among the neighboring and the further neighboring planes of ferromagnetically-aligned moments. A modification of these interactions by magnetic field, pressure, impurity, etc., will drastically influence the helical state and consequently the interplay between magnetism and superconductivity.

Keywords: $HoNi_2B_2C$, helimagnetism, magnetoresisivity, field-induced phase transitions.

1. INTRODUCTION

Resistivity [1,2], specific heat [3], neutron diffraction [4,5], pressure [6] and magnetization [3,7] studies on the superconducting ($T_c \approx 7.5K$) $HoNi_2B_2C$ characterized its low-T magnetic properties as follows: crystal field effects force the Ho moments along the ab-plane (with negligible in-plane anisotropy) leading to anisotropic paramagnetic susceptibilities below 100K. The planar Ho-moments have strong ferromagnetic (FM) intraplanar coupling and relatively weak antiferromagnetic (AFM) interplanar couplings. The latter couplings lead to an AFM transition ($T_N = 5K$) with an accompanying helical state. The helical state, which plays a decisive role in the interplay between superconductivity and magnetism, is energetically unstable at $T<4.7K$ and transforms into a commensurate AFM state.

The single-crystal high field magnetization (H applied along the easy plane, $T< 5K$) reveals a cascade of three phase transitions [3]. For low-T, the first transition occurs at $H_1 \approx 3.8$ kOe where almost one third of the total magnetic moment is oriented along the field direction, the second transition at $H_2 \approx 8.6$ kOe where two thirds of the magnetic moment is along the field direction. Almost full saturation is reached at $H_3 \approx 13.2$ kOe

In this communication we discuss the formation of the helical state and the features of the H-T magnetic phase diagram of $HoNi_2B_2C$. In addition, we show new experimental results that confirm the findings of the single-crystal magnetization measurements. The formation of this helical state (Sec.2) is

related to the competition between the interplanar long-range AFM interactions. Furthermore, the influences of the physical parameters (pressure[6], applied magnetic field[1-5], sample inhomogeneity[6], etc.) on the reentrant state are related to their influence on the RKKY interactions. Our discussion of the H-T phase diagram (Sec.3) is based on the following assumption: on the application of an external magnetic field, the AFM superconducting state is unstable against a distorted helical state. The field-induced transitions (and the derived H-T phase diagram) are then a consequence of the well-studied influence of the applied field on the (distorted) helical spin structure [8]. Finally, we report in Sec.4 a novel longitudinal magnetoresistivity of $HoNi_2B_2C$ (at the helical region and in fields up to 80 kOe). The $\Delta\rho(H) = \{\rho(H)-\rho(H=0)\}/\rho(H=0)$ showed three magnetic phase transitions in agreement with the reported H-T phase diagram [3].

2. THE FORMATION OF THE HELICAL STATE AND ITS RESPONSE TO AN EXTERNAL FIELD.

A collection of RKKY-coupled moments with a large and positive out-of-plane (c-axis) D anisotropy, in an applied field H along the a-axis, can be described by the following Hamiltonian [8]:

$$H = -\sum_{m,n(m\neq n)} J(\vec{R}_{nm})\vec{S}_n\vec{S}_m + D\sum_n (S_n^c)^2 + g\mu_B H\sum_n S_n^a \qquad (1)$$

where $\vec{S}$ denotes the total angular moment. The other symbols have their usual meanings.

Depending on the strength of the $J(R_{nm})$, the solution of Eq.1 predicts three stable ordered spin configurations: the FM, the AFM and the helical state [8]. Without loss of generality, let us assume that the $J(R_{nm})$, D, S and R_{nm} are given by the structural-chemical properties of $HoNi_2B_2C$. For this compound, it will be shown below that the lowest magnetic ground state *is* a helical state (the observed transformation into an AFM state at lower temperatures [4,5] is discussed below). A small external field will distort the helical state such that the spiral angle ϕ_n, at the n^{th} plane, to first order in H is given by :

$$\phi_n = \frac{nQc}{2} - \frac{g\mu_B SH \sin(\frac{nQc}{2})}{S^2[2J(\vec{Q}) - J(0) - J(2\vec{Q})]} \qquad (2)$$

where $J(Q)$ is a Fourier transform of $J(R_{nm})$ at wave vector Q, and c is the chemical cell parameter. Eq.2 shows that the spiral angle does not depend explicitly on the anisotropy factor D; i.e., the planar anisotropy is not necessary for the formation of the helical state.

A further application of the external field will transform the helical state into the saturated FM state through a set of field-induced magnetic phase transitions. The number of such transitions may vary depending on the strength of the exchange parameters, anisotropic factors and magnetostriction, etc. At these intermediate states, the so-called fan structures, the magnetic moments oscillate around a fixed direction [8].

On the experimental side, the influence of an applied magnetic field on a helical ground state had been extensively studied [8]. As an example, the

magnetic ground state of the Ho metal is a helical structure between 20K and 133K. Above this range of temperatures, the metal is paramagnetic while below that range it has a conical spin ordering. In the helical state, the application of a magnetic field, along the Ho-metal easy axis, leads to a cascade of magnetic phase transformations: the low-field helical structure transforms into the high-field FM arrangement through a set of intermediate fan structures.

Now, we show that the conditions (required by Eq.1) for the formation of the helical state are satisfied in the $HoNi_2B_2C$ compound. Let us assume that the anisotropy D and the intraplanar FM couplings in Eq.1 are large enough so that the Ho-moments within each plane form a FM sheet. Further, let us consider the interplanar RKKY exchange forces only among the first and the second nearest planes [9] denoted, respectively, by J_{o1} and J_{o2}. This is equivalent to a magnetic chain having nearest (J_{o1}) and next-nearest (J_{o2}) interactions (see Fig.1). From Eq.1, the zero-field stable ordered configurations are given by the condition

$$|J_{o1} + 4J_{o2}\cos(\phi_1)|\ \sin(\phi_1) = |J_{o1} + 4J_{o2}\cos(Qc/2)|\ \sin(Qc/2) = 0 \qquad (3)$$

where ϕ_1 is the zero-field spiral angle (Eq.2). Eq.3 reiterates the previously mentioned statements: there are three magnetic ground states; the FM state when $Q = 0$, the AFM state when $Q = 2\pi/c$ and the helical state when

$$J_{o1}, J_{o2} < 0 \text{ and } \quad J_{o1}/J_{o2} = -4\cos(\phi_1) < 4. \qquad (4)$$

For $HoNi_2B_2C$, this conditions are satisfied because :

$$J_{o1}/J_{o2} = -4\cos(\phi_1) = -4\cos(16.4°+180°) \approx 3.84, \quad (5)$$

where the substituted value of the spiral angle, ϕ_1, is taken from Ref.4. It is worth remembering that for an electron gas polarized by a plane of ferromagnetic aligned moments, the polarization strength decays with an $1/(r^2)$ dependence (where $r = c/2$ is the interplanar separation). This dependence yields $J_{o1}/J_{o2} \approx 4$ in good agreement with the value determined by substituting the experimental parameters in Eqs.4-5.

In the above analysis, the helical state is shown to be energetically favorable at lower temperatures. However, it is shown experimentally [1-6] that below 4K, superconductivity is fully restored and coexists with a commensurate AFM order. Such type of transformation (from helical into AFM) may be due to the competition between the helical order and the superconductivity and/or a temperature-dependent variation in the parameters of the Hamiltonian (Eq.1). Magnetostriction and ab-plane anisotropy may be additional factors. It is worth mentioning that, in the Ho metal, the planar anisotropy and the magnetostriction are affecting the low-T transformation of the helical structure into the conical state [8].

Clearly, the AFM interplanar RKKY couplings which extend beyond the nearest neighboring planes drive the system into the helical state. Consequently any physical factor that affects these interactions influences the helical state and

thus influences the interplay between magnetism and superconductivity. Clear demonstrations of these effects were given by the pressure [6], magnetization [3,6,7] and magnetoresistive studies[2]. Another illustration is the experimental fact that the reentrant behavior is strongly sensitive to the presence of impurities [6] such as foreign phases, intergrowth, defects, sample inhomogeneity, etc. The impurity influences are equivalent to random modifications in the magnetic RKKY bonds and as such, they will inhibit the establishment of the helical state. This explains the observation of Schmidt et al [compare Figs.3-4 in Ref.6] that in a contaminated (impure) sample, the reentrant behavior was quenched or quasi-quenched while the superconducting transition was increased by 1K [11].

3. THE CASCADE OF FIELD-INDUCED PHASE TRANSITIONS IN $HoNi_2B_2C$.

If the low-T AFM ground state in $HoNi_2B_2C$ is stable under an external in-plane magnetic field ($>H_2$), then a spin flop transition (with the moments perpendicular to H) will occur at a critical field H_{sf} and the magnetization isotherms above H_{sf}, must evolve as [9,10] :

$$M/M_S = H/(2H_{ex}-H_a) \approx H_{ap}/(2H_{ex}) \qquad (6.a)$$

$$H_{sat} = (2H_{ex}-H_a) \approx 2H_{ex} \qquad (6.b)$$

$$H_{sf} = \sqrt{(2H_aH_{ex}-H_a^2)} \qquad (6.c)$$

where, H_{ex} , H_a , H_{sat} and H_{sf} are, respectively, the interplanar exchange field, the in-plane anisotropy field ($<< 2H_{ex}$), the saturation field and the spin-flop field. M_S is the sublattice magnetization ($\frac{1}{2}Ng\mu_B S$).

As demonstrated in Ref.3 (shown in Fig.2), the easy plane magnetization of $HoNi_2B_2C$ did not show such a behavior. It is tempting to assume that the AFM state is not stable for magnetic field higher than H_{c2}. Rather, it transforms into a distorted helical structure with a spiral angle as given by Eq.2. Then, the reported magnetization isotherms (Fig.2, middle) and the derived H-T phase diagram (Fig.2, right) can be discussed (and assigned) in terms of the theoretical arguments given in Sec.2. The field induces, firstly, a phase transition at H_1 from the distorted helical ground state to a fan structure (type-I). Secondly, a phase transition at H_2 from a fan structure (type-I) to a fan structure (type-II). Finally, a phase transition at H_3 from the fan structure (type-II) to the FM saturated state.

The facts that the zero-field ground state at $4.7K < T < 5K$ is the helical state (with similar field-induced magnetization jumps) and that this helical state is energetically close to the AFM state provide extra supports to the assumption that for $H_{c2}<H<H_1$, the superconducting AFM state is transformed into a distorted helical state (see Fig.2).

4. MAGNETORESISTANCE EVIDENCES OF THE FIELD-INDUCED MAGNETIC PHASE TRANSITIONS IN $HoNi_2B_2C$.

As well known, magnetoresistivity can provide an invaluable information on field-induced magnetic phase transitions [see e.g. 8]. It can readily be used to construct an H-T phase diagram with reasonable agreement with other techniques such as neutron diffraction and magnetization. The magnetoresitivity of some of the RNi_2B_2C compounds had been measured in field up to H_{c2}[see e.g. 2]. We are particularly interested in studying this effect in higher fields ($H > H_{c2}$) so as to confirm the H-T phase diagram and to check the validity of the picture we proposed for the formation of the helical state.

Samples were prepared according to the standard argon arc-melt procedures [1-6]. Room-temperature structural characterization was carried out in standard CuKα diffractometer. The longitudinal magnetoresistivity (j // H) was measured on a bar of a polycrystalline sample in fields up to 80 kOe using the four-point dc method. The sample temperature was monitored by Carbon glass thermometer with its long axis set perpendicular to the field direction. Temperatures were corrected for the magnetic field's influence following the procedure described in Ref.11.

The XRD diffractogram (shown indexed in Fig.3) demonstrates that the majority phase (>90%) is the tetragonal I4/mmm $HoNi_2B_2C$ phase and with the following lattice parameters: a = 3.520(2)Å, c =10.521(2)Å. As clearly to be seen from Fig.3, the sample is well textured and the c-axis is the preferred

orientation. Physical characterization showed $T_c \approx 8K$ and a quasi-reentrant feature. The weakening of the reentrant behavior is attributed to the presence of small impurity (marked with x in Fig.3) which, as discussed above, influences destructively the formation of the helical state.

A typical curve of the $\Delta\rho(H)$ is shown in Fig.4. As evident, the $\Delta\rho(H)$ and the magnetization jumps are following each other. Moreover, $\Delta\rho(H)$ reaches its minimum saturated value when the magnetic saturation occurs. From Fig.4, the estimated critical fields are: H_1=3.4(3) kOe, H_2=8.5(5) kOe, H_3=12.8(4) kOe. These agree qualitatively with the reported critical fields [3]: $H_1 \approx 3$ kOe, $H_2 \approx 7$ kOe and $H_3 \approx 12$ kOe.

Although, the sample is a polycrystal and is contaminated with a minority impurity phase, nevertheless, the results confirmed unambiguously the single-crystal magnetization results and the H-T phase diagram [3]. This agreement is sketched in Fig.2. In fact, the H-T phase diagram is lending a transparent interpretation for the magnetoresistivity features. In a first approximation, the anomalous magnetoresistivity is related to the thermally averaged magnetic moment $\langle\mu\rangle$ by the following relation [8]:

$$\Delta\rho(H) = \{\rho(H)-\rho(H=0)\}/\rho(H=0) \propto -\langle\mu\rangle^2 \qquad (7)$$

Comparison of Eq.7 with the experiments is not attempted because of the polycrystalline form of the samples. The saturation of the magnetization of a (textured) sample implies that all the spins of the randomly oriented ab-planes

are aligned along the field direction. Therefore, the anisotropic field H_a (and the strength of the anisotropy parameter D) must satisfy the following: $H_a \leq H_{sat}$.

Fig.5 shows that at least 78% of the magnetic incoherent resistive scattering is removed on applying a small magnetic field (~ 1.327 kOe), in agreement with the magnetoresistivity results of Eisaki et al [2]. From Eq.7, this corresponds to an 88% of the full magnetic alignment. In addition, in these low-fields ranges, the $\Delta\rho(H)$ can be described by (see inset of Fig.5):

$$\Delta\rho(H) = 0.068[\sin(H/0.089)]^2 \qquad (8)$$

Such a functional dependence is reminiscent of the behavior observed in ferromagnetic materials where the applied field influences $\Delta\rho(H)$ through the reorientation of the magnetic domains. In the absence of good single crystal, we can not exclude the possibility that this fast drop in $\Delta\rho(H)$ is related to the low-field fast saturation of the impurities' magnetization.

5. CONCLUSION

The helical state in $HoNi_2B_2C$ is shown to arise from the competing character of the long-range interplanar AFM couplings. At lower temperatures, the competition between magnetism and superconductivity provides an extra energy term that may stabilize the commensurate AFM state. The application of

a magnetic field at T < 4.7K leads to the destruction of the Cooper pairs and thus provides additional electrons to intermediate the interplanar magnetic coupling. We argued that the resulting magnetic ground state is a distorted helical structure. Further application of the field induces a phase transition at H_1 from the (distorted) helical state to a fan structure (type-I), then a phase transition at H_2 from a fan-I to a fan-II structure and finally a phase transition at H_3 from the fan-II to the FM saturated state.

The magnetoresistivity measurement on $HoNi_2B_2C$ in the reentrant (helical) region revealed a cascade of three magnetization jumps in agreement with the H-T phase diagram derived from the single-crystal magnetization studies. Single-crystal magnetoresistivity studies on the magnetic RNi_2B_2C may be used to map out the H-T phase diagram and to address the low-T field-induced instability of the AFM state against a distorted helical state.

Acknowledgment: Prof. M. A. Continentino and W. Baltensperger are sincerely thanked for their interests, helpful discussions and critical readings. R. Pereira is thanked for taking the XRD diffractogram.

REFERENCES

1. R. J. Cava, H. Takagi, B. Batlogg, H. W. Zandbergrn, J. J. Krajewski, W. F. Peck, Jr, T. Siegrist, B. Batlogg, R. B. van Dover, R. J. Felder, K. Mizuhashi, J. O. Lee, H. Eisaki, and S. Uchida, Nature 367(1994)252.
2. H. Eisaki, T. Takagi, R. C. Cava, B. Batlogg, J. J. Krajewski, W. F. Peck , K. Mizuhasi, J. O. Lee and S. Uchida, Phys. Rev. B 50(1994)647.
3. P. C. Canfield, B. K Cho, D. C. Johnston, D. K. Finemore, M. F. Hundley, Physica C 230 (1994) 397.
4. T. E. Grigereit, J. W. Lynn, Q. Huang, A. Santoro, R. J. Cava, J. J. Krajewski and W. F. Peck, Jr, preprint;
5. A. I. Goldman, C. Stassis, P. C. Canfield, J.Zarestky, P. Dervenagas, B. K. Cho and D. C. Johnston Phys. Rev. B 50 (1994) 9668.
6. H. Schmidt and H. F. Braun, Physica C in press.
7. M. El Massalami, B. Giordanengo, S. L. Bud'ko, and E. M. Baggio-Saitovitch, Physica C in press.
8. B. Coqblin , The Electronic Structure of Rare-Earth Metal and Alloys: the Magnetic Heavy Rare-Earth (Academic Press, London, 1977).
9. J. S. Smart, Effective Field Theories of Magnetism ,(W.B.Saunders Company, (1966).
10. R. L. Carlin and A. J. van Duyneveldt, Magnetic Propeties of Transition Metal Compounds, (springer-Verlag, N.Y.,1978).
11. H. H. Sample, B. L. Brandt and L. G. Rubin, Rev. Sci. Instrum. 53 (1982) 1129.

FIGURES CAPTIONS

Fig.1 The linear chain equivalent of the helical state in the $HoNi_2B_2C$ compound. The ferromagnetic planes are perpendicular to the chain axis. The periodicity is across 22 HoC planes[4]. The nearest neighbor exchange coupling is J_{o1} while the next nearest neighbor coupling is J_{o2}.

Fig.2 An idealized sketch of the low-T magnetic properties of the $HoNi_2B_2C$. *Left*: the $\Delta\rho(H)$ versus H at the reentrant region (see text and Fig.4). *Middle*: is the magnetization versus H at the low-T region, H is along the easy plane (adapted from Ref.3). *Right*: is the H-T phase diagram (Ref.3). The assignment of the field-induced magnetic phases is as follows: **Fan-I (Fan-II)** denotes the fan structure of type-I (type-II), **s.c.+afm** denotes the superconducting commensurate antiferromagnetic phase and **helical** denotes the (distorted) helical state. $\mathbf{H_n}$ denotes the critical field that induces the n^{th} magnetization jump.

Fig.3. Room temperature Cu-K_α X-ray diffractogram of a polycrystalline sample of $HoNi_2B_2C$. The strong peaks of an unidentified phase are marked with an x. The c-axis is the preferred orientation.

Fig.4 The longitudinal magnetoresistivity versus field of the polycrystalline $HoNi_2B_2C$ in the helical region (T=4.7(2) K). The inset demonstrates the three phase transitions. For this curve, the sample was field-cooled in 80 kOe. After stabilizing the temperature at 4.7K, the measuring points were taken on decreasing the magnetic field.

Fig.5 emphasizes the low-field squared-sinusoidal functional dependence.

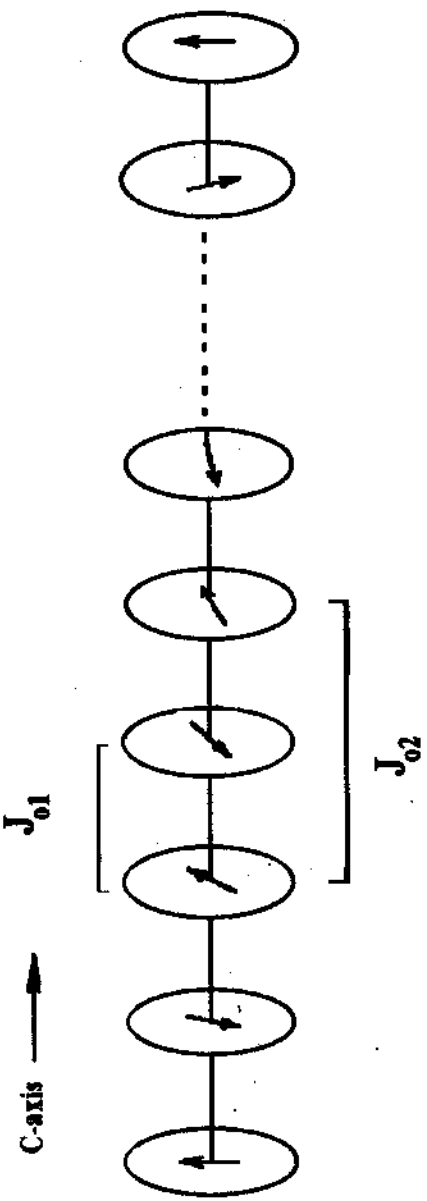

Fig.1

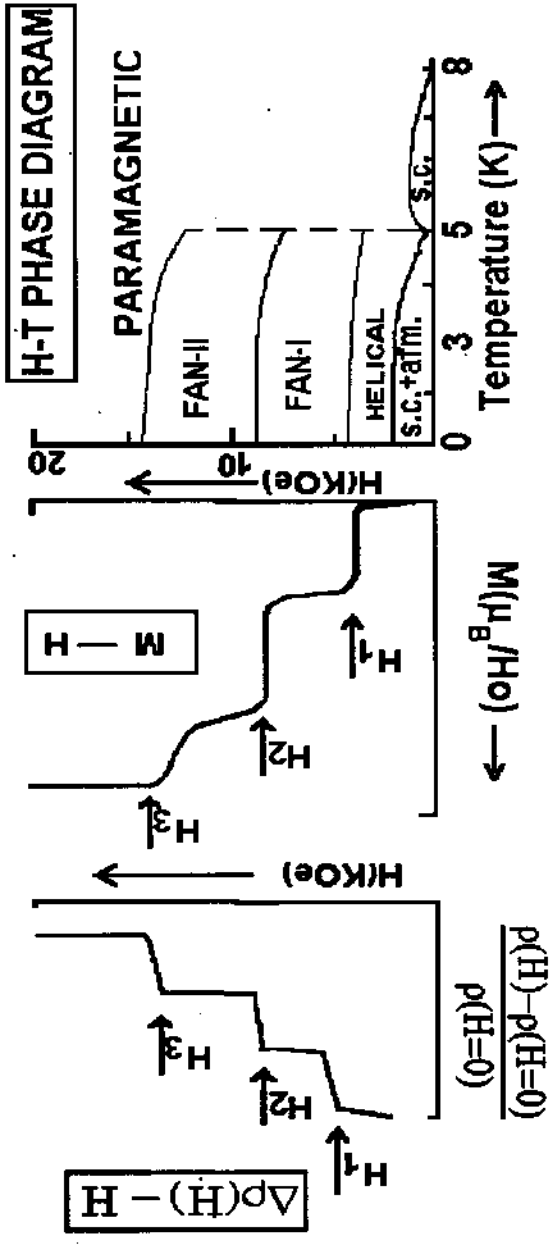
H-T PHASE DIAGRAM
PARAMAGNETIC
FAN-II
FAN-I
HELICAL
s.c.+atm.
s.c.
0
3
5
8
Temperature (K)
20
10
H(KOe)
M — H
H1
H2
H3
M(μB/HO)
H(KOe)
Δρ(H) − H
H1
H2
H3
ρ(H)−ρ(H=0) / ρ(H=0)

Fig.2

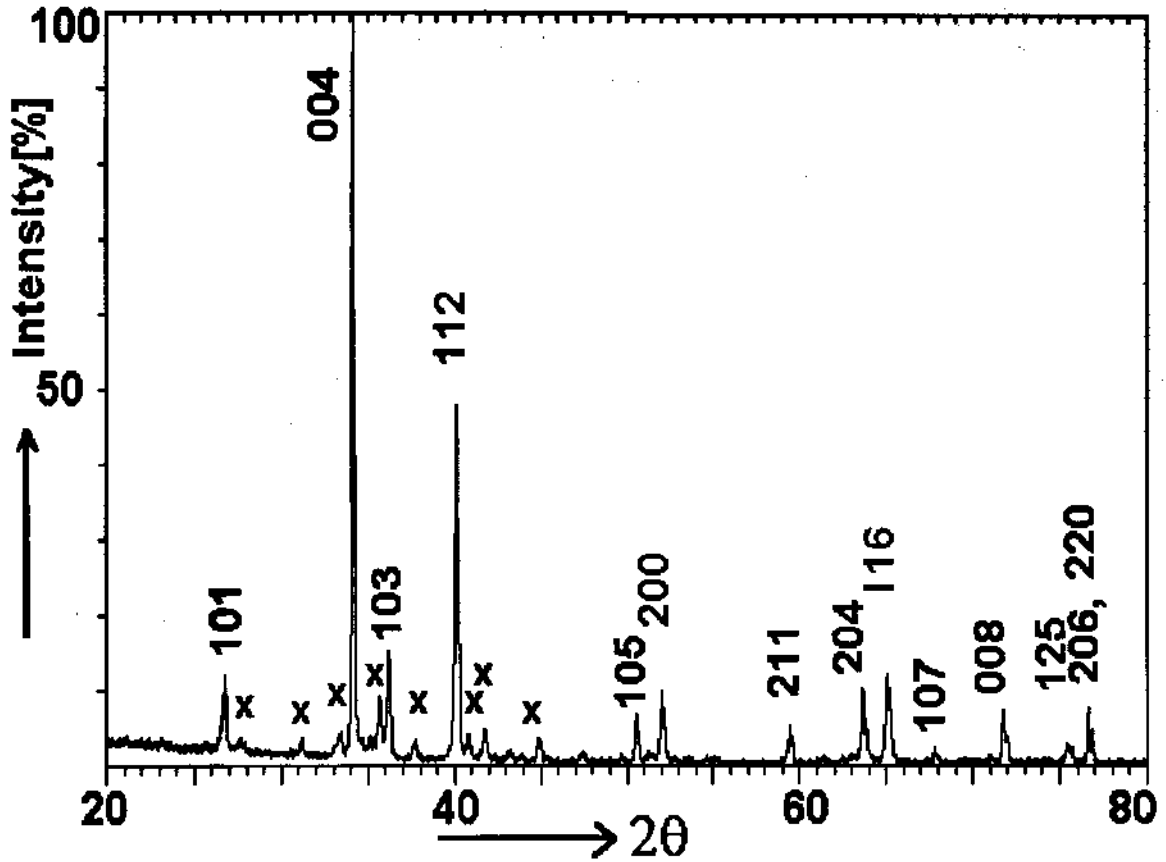
100
50
Intensity[%]
004
112
101
103
105
200
211
204
116
107
008
125
206, 220
x
20
40
60
80
2θ

Fig.3

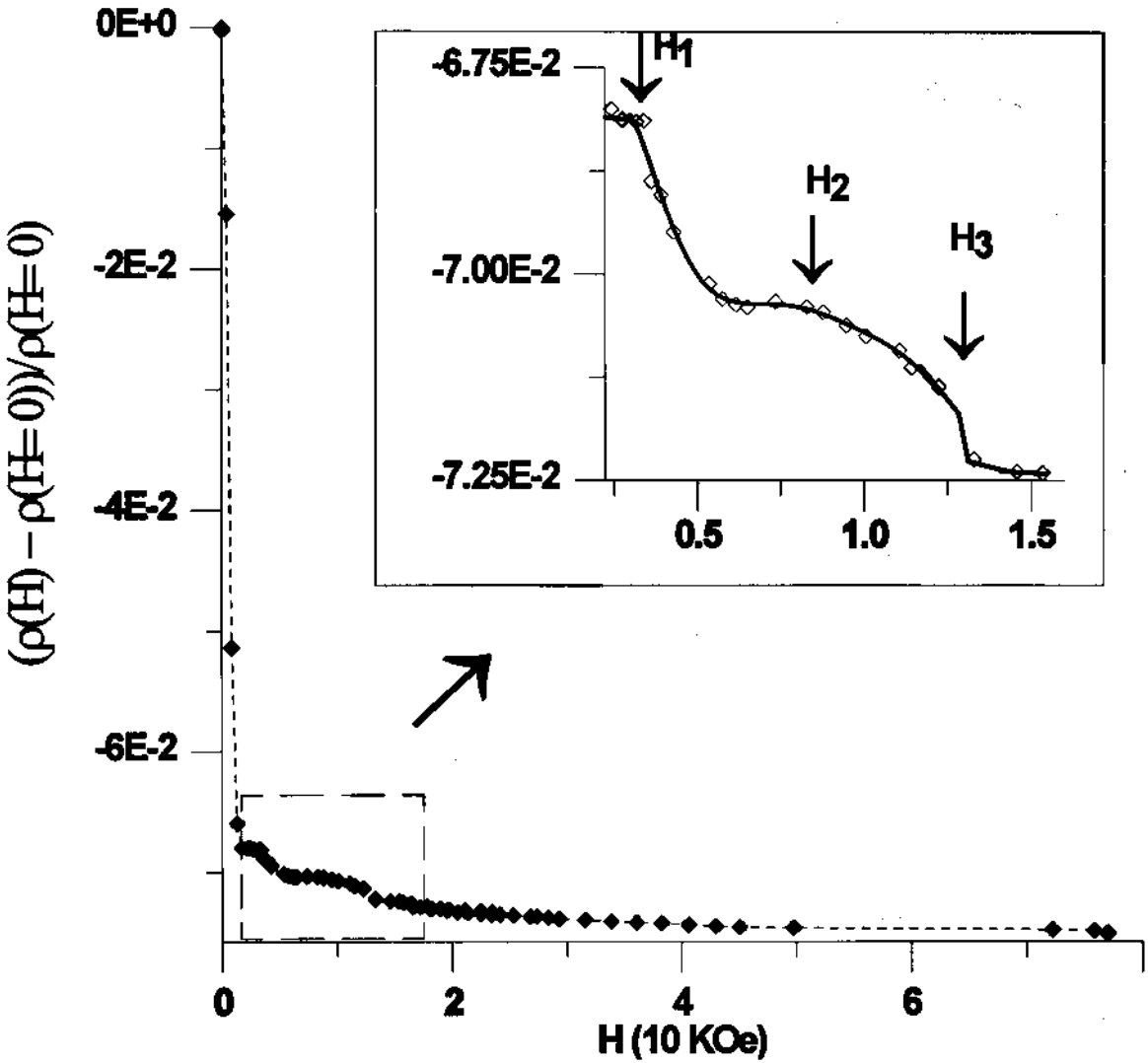
0E+0
-2E-2
-4E-2
-6E-2
(ρ(H) – ρ(H=0))/ρ(H=0)
0
2
4
6
H (10 KOe)
-6.75E-2
-7.00E-2
-7.25E-2
H1
H2
H3
0.5
1.0
1.5

Fig.4

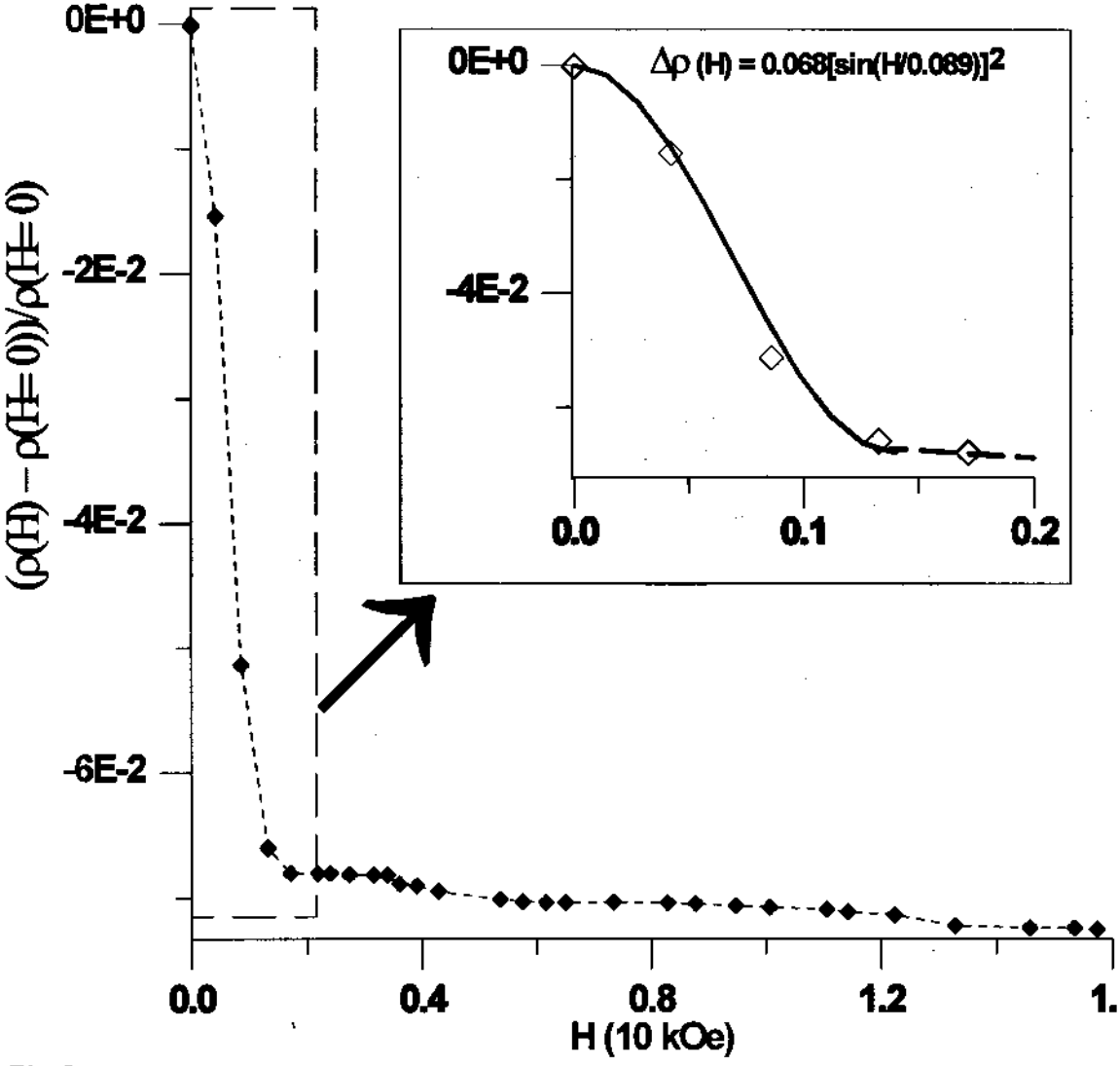
0E+0
-2E-2
-4E-2
-6E-2
(ρ(H) – ρ(H= 0))/ρ(H= 0)
0.0
0.4
0.8
1.2
1.
H (10 kOe)
0E+0
-4E-2
Δρ (H) = 0.068[sin(H/0.089)]2
0.0
0.1
0.2

Fig.5